Liquid Crystals
Publication details, including instructions for authors and subscription information:
http://www.informaworld.com/smpp/title~content=t713926090

Rich polymorphism in 4-propyl-4'-thiocyanato-1,1'-biphenyl (3TCB) revealed by adiabatic calorimetry

R. Pełka[ab]; Yasuhisa Yamamura[a]; M. Jasiurkowska[b]; M. Massalska-Arodź[b]; Kazuya Saito[a]
[a] Department of Chemistry, Graduate School of Pure and Applied Sciences, University of Tsukuba, Tsukuba, Ibaraki 305-8571, Japan [b] The Henryk Niewodniczański Institute of Nuclear Physics Polish Academy of Sciences, Kraków, 31-342, Poland

To cite this Article Pełka, R. , Yamamura, Yasuhisa , Jasiurkowska, M. , Massalska-Arodź, M. and Saito, Kazuya(2008) 'Rich polymorphism in 4-propyl-4'-thiocyanato-1,1'-biphenyl (3TCB) revealed by adiabatic calorimetry', Liquid Crystals, 35: 2, 179 — 186
To link to this Article: DOI: 10.1080/02678290701819181
URL: http://dx.doi.org/10.1080/02678290701819181

Liquid Crystals,
Vol. 35, No. 2, February 2008, 179–186

Taylor & Francis
Taylor & Francis Group

Rich polymorphism in 4-propyl-4′-thiocyanato-1,1′-biphenyl (3TCB) revealed by adiabatic calorimetry

R. Pełka[ab]*, Yasuhisa Yamamura[a], M. Jasiurkowska[b], M. Massalska-Arodź[b] and Kazuya Saito[a]

[a]*Department of Chemistry, Graduate School of Pure and Applied Sciences, University of Tsukuba, Tsukuba, Ibaraki 305-8571, Japan;* [b]*The Henryk Niewodniczański Institute of Nuclear Physics Polish Academy of Sciences, Radzikowskiego 152, Kraków, 31-342, Poland*

(Received 1 October 2007; final form 20 November 2007)

The thermal behaviour of 4-propyl-4′-thiocyanatobiphenyl (3TCB) was studied by adiabatic calorimetry. In addition to the isotropic liquid and smectic E (SmE) phases, five crystalline phases were detected. Such a rich polymorphism was not observed for the other low-*n* members of the *n*TCB homologous series (*n*=2–5). The observed anomalies are analysed and the possible origin for their existence is suggested. The temperature quench of the SmE phase leads to a metastable crystalline state with a multiple-stage relaxation process.

Keywords: smectic E phase; soft matter; adiabatic calorimetry; polymorphism

1. Introduction

In some materials with elongated molecules a smectic E (SmE) phase is found, often called a ''soft smectic crystal''. It is known to have an orthogonal structure with ''herring bone'' ordering of the molecules in its layers (*1–5*). In previous studies, including dielectric (*6–9*), ^{2}H NMR (*10*), quasielastic neutron scattering (*11, 12*), adiabatic calorimetry and ^{1}H NMR measurements (*13*), the molecular reorientations around the short molecular axis, flipping motions of phenyl rings, translational diffusion and libration around the long molecular axis were detected. Complementary experimental methods point out that in the SmE phase the flip-flop rotations around the short molecular axis are most sensitive to the arrangement of molecules, which is characterised by a relatively high activation barrier (*6, 8, 13*). In the deeply supercooled SmE phase of the 4-butyl-4′-isothiocyanato-1,1′-biphenyl (4TCB), methyl reorientations were shown to be the only dominant molecular motions (*13*). The motions were also detected in the ordered crystalline phase of 4TCB obtained after laborious preparations. Although many details of the molecular dynamics have been revealed so far (*1–13*), the role of disorder in the SmE phase remains unclear. To investigate how the length of alkyl chains affects cooperative behaviour in mesogenic compounds and influences its polymorphic behaviour is of considerable interest and requires further experimental and theoretical effort. The present paper reports a study of the thermodynamic features down to 6 K and, concomitantly, the details of the solid-state polymorphism of 3TCB. It is the next compound below 4TCB belonging to the series of 4-*n*-alkyl-4′-isothiocyanoto-1,1′-biphenyls (C_nH_{2n+1}–C_6H_4–C_6H_4–NCS), abbreviated as *n*TCB, which are known to exhibit a SmE phase around room temperature for *n*=2–12 (*6, 14*). The goal was to compare the adiabatic calorimetry results of 3TCB with those obtained for 4TCB and 5TCB. It has been shown by adiabatic calorimetry that in 4TCB one crystalline phase exists and in 5TCB two crystalline phases are found in addition to the isotropic liquid and SmE phases (*15*).

2. Experimental

The 3TCB sample was kindly supplied by Prof. R. Dąbrowski, The Military University of Technology in Warsaw (*16*) and used as obtained for thermal measurements. At room temperature the sample is in a crystalline phase.

Heat capacity measurements were performed on heating using a laboratory-made adiabatic calorimeter, the details of which are described elsewhere (*17*). The measurement was carried out by the so-called intermittent-heating adiabatic method. The sample was loaded into a gold-plated calorimeter vessel. The vessel was evacuated for 1 h and sealed after introducing a small amount of helium gas (10^5 Pa at room temperature), which serves as heat conduction gas inside the vessel. The mass of the sample was 1.4496 g (5.7214 mmol) after buoyancy correction. The sample contributed to the total heat capacity by 18% at 50 K, 14% at 100 K, 17% at 200 K, 20% at 300 K and 25% at 365 K. The working

*Corresponding author. Email: robert.pelka@ifj.edu.pl

ISSN 0267-8292 print/ISSN 1366-5855 online

DOI: 10.1080/02678290701819181
http://www.informaworld.com

thermometer was a platinum resistor (MINCO, S1059), the temperature scale of which is based upon the ITS-90.

A supplementary differential scanning calorimetry (DSC) measurement was carried out using the Perkin Elmer DSC Pyris 1 instrument in the temperature range 93–338 K and using a scan rate of 10 K min^{-1}. Prior to the measurement the 3.97 mg sample was heated up to 338 K to ensure its conversion into the SmE phase.

3. Results and discussion

Heat capacity and phase transitions

The heat capacity of 3TCB was measured between 6 and 370 K by adiabatic calorimetry in numerous experimental runs for various thermal treatments of the sample. The temperature increment due to each energy input may be deduced from the adjacent mean values of temperature. Typical heat capacity, $C_p(T)$, data are shown in Figure 1 for the whole temperature range studied: open circles are the data measured after initial cooling from room temperature (first measurement series), whereas solid circles correspond to the data obtained for the sample cooled down to liquid He temperature (at a rate of 2 K min^{-1} around the melting point), after it was heated above the crystal–SmE phase transition (second measurement series).

During the first measurement series a continuous $C_p(T)$ measurement from 80.9 K up to 300.4 K was performed and four anomalies were observed around 102, 115, 190 and 259 K. Next, repeated measurements were performed around the anomalies at 259 and 190 K, with the aim of studying supercooling effects. Thereafter, the sample was cooled to liquid He temperature (at an average rate of 1.5 K min^{-1}) and the measurement was performed from 6.7 K up to 121.2 K. Then the sample was cooled down to 101.8 K to check the existence of the supercooling effect for the anomaly at 102 K.

The second measurement series started after the sample was melted once above 303 K. It was then cooled to liquid He temperature at a rate of 2 K min^{-1} around the melting point. The measurement was continued up to 289.6 K. Next, on applying the fractional heating method around the ordered crystal–SmE anomaly, the measurement was continued until the transition to the isotropic (I) liquid phase was passed.

The $C_p(T)$ measurements revealed in 3TCB a rich polymorphism in the solid state. The largest anomaly due to the SmE–I transition was observed at 362.92 K with a latent heat of 11.75 kJ mol^{-1}. Below the melting temperature, T_m=303.7 K, there are two peaks and a broad hump in the heat capacity curve dividing the temperature range into five regions. Here we aim to provide a thermodynamic description of the transitions between crystalline phases designated by symbols C1–C5, as is shown in Figure 1.

The hump observed in the temperature range 80–120 K was well reproduced in several experimental runs (see Figure 2): open circles denote the measurement starting from liquid N temperature; solid circles the measurement from 6 K; open triangles the data obtained in the measurement from 101.8 K. Assuming a normal heat capacity as a curve interpolating

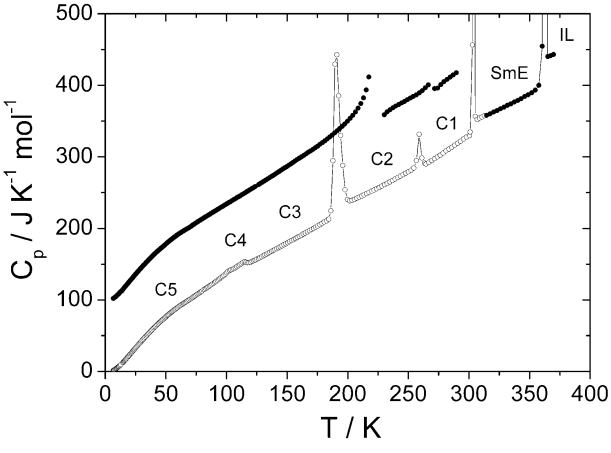

Figure 1. Measured molar heat capacity of 3TCB. Open circles denote data obtained in the first measurement series after initial cooling from room temperature (at an average rate of 1 K min^{-1}); solid circles correspond to the data obtained in the second measurement series for the sample once heated above 303 K and cooled to liquid He temperature (the cooling rate around the melting point was about 2 K min^{-1}). For clarity the data points of the second series below the C1–SmE transition are shifted vertically by 100 J K^{-1} mol^{-1}.

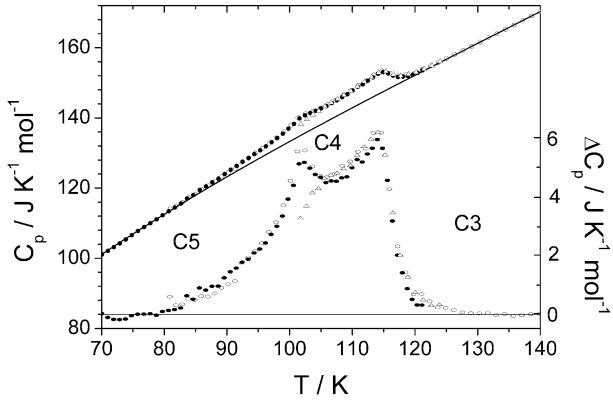

Figure 2. Measured heat capacities and excess heat capacities of 3TCB around two successive phase transitions at 102 K and 115 K. Different symbols denote the data obtained in different runs of measurement. The solid curve in the upper part is the baseline assumed.

smoothly between the high and low temperature region (the least square fit of the third order polynomial was applied), the excess heat capacity gives rise to two distinct maxima at about 102 K and 115 K, which may be regarded as phase transition temperatures. The integration yields the combined excess enthalpy and entropy associated with the anomalies of $119 \pm 8\,\mathrm{J\,mol^{-1}}$ and $1.14 \pm 0.07\,\mathrm{J\,K^{-1}\,mol^{-1}}$, respectively, where the errors were estimated using the two independent runs. By drawing a tentative baseline for the lower temperature anomaly its contributions to the excess quantities are estimated to be about 9% of their combined values. The magnitude of the total entropy change is much smaller than that expected for a typical order–disorder phase transition ($R\ln 2 \approx 5.8\,\mathrm{J\,K^{-1}\,mol^{-1}}$), which suggests that each transition is of a displacive type. For the lower temperature anomaly the supercooling can be realised as plotted by the open triangles, which indicates its first order character. This anomaly is superimposed on the low-temperature tail of the second anomaly accompanied neither by latent heat nor showing a considerable diverging trend. This indicates that the corresponding phase transition is of a higher order with an insignificant fluctuation effect. Since the structural information is unavailable for all crystalline phases, it is, at present, difficult to discuss further the nature of this phase transition. A similar double hump anomaly was reported around 140 K for phenazine-chloranilic acid (*18*). Similarly, the character of the lower temperature anomaly was demonstrated to be of first order. The anomaly was supposed there to be due to the successive phase transitions related to the phase sequence including the incommensurate phase, i.e. normal phase–incommensurate phase–commensurate phase, on cooling (*19*).

All transitions observed above the double-peak anomaly displayed supercooling. For each of these transitions a jump in heat capacity due to different baselines was clearly recognised, which allowed the corresponding excess enthalpies and entropies to be estimated. The results are summarised in Table 1,

Table 1. Thermodynamic quantities associated with phase transitions in 3TCB.

Anomaly	T_{trs}/K	$\Delta_{trs}H$/ kJ mol^{-1}	$\Delta_{trs}S$/ J K^{-1} mol^{-1}
C5–C4 transition	102	0.12	1.14
C4–C3 transition	114		
C3–C2 transition	191.27	1.3	6.8
C2–C1 transition	259.0	0.15	0.57
C1–SmE	303.7 (304.8)	7.02 (9.16)	23.1
SmE–IL	362.92 (361.35)	11.75 (14.77)	32.4

The DSC results reported by Urban *et al.* (*6*) are shown in parentheses.

together with the DSC results reported by Urban *et al.* (*6*) shown in parentheses.

The values obtained for the enthalpy and entropy of C1–SmE transition of 3TCB are lower than those found for its analogue in 4TCB ($9.567\,\mathrm{kJ\,mol^{-1}}$ and $33.67\,\mathrm{J\,K^{-1}\,mol^{-1}}$, respectively, at 284.1 K) (*13*). This can be attributed to the difference in the number of degrees of freedom associated with molecules of these homologues. The entropy of the transition amounts to about two-thirds of the entropy of fusion of the SmE phase for 3TCB, whereas for 4TCB it has been found to be almost the same (*13*). The fact that both values are comparable demonstrates (in terms of entropy) that the molecular order in the SmE phase falls somewhere in between the solid state and isotropic liquid. At the same time, the relatively smaller value of entropy observed for the C1–SmE phase transition is due to the fact that the conformational motions of the shorter alkyl chain of 3TCB result in a more restricted rotational freedom in the SmE crystal-like phase. This is consistent with the substantial increase of activation enthalpy for rotations around the short molecular axis for the *n*TCB homologous series with shortening the alkyl chain below $n=5$ with a maximum at $n=3$ observed in dielectric studies (*6*).

The entropy jump due to the transition from C3 phase to C2 phase was estimated to be $6.8\,\mathrm{J\,K^{-1}\,mol^{-1}}$, which is close to the value of $R\ln 2$ ($\approx 5.8\,\mathrm{J\,K^{-1}\,mol^{-1}}$) corresponding to the contribution from the Ising-spin-like degrees of freedom. This suggests the possibility that beside a lattice adjustment the transition involves a head-to-tail ordering of molecules. To settle this conjecture further experiments involving X-ray, dielectric or NMR studies are needed.

Primary heat capacity data were smoothed out using a cubic spline procedure in subsequent appropriately chosen temperature regions between the anomalies. Standard thermodynamic quantities such as enthalpy function, entropy increment and the Gibbs energy function were obtained from appropriate integration of the resulting fits. In the calculation, the crystalline phase C5 was assumed to obey the third law of thermodynamics, as there is no anomaly in the temperature dependence of heat capacity down to the lowest temperature accessible experimentally (6 K). In order to estimate the values of C_p below $T=6$ K we extrapolated the experimental values assuming a polynomial in temperature. The least square fitting to 13 data points located in the temperature range of 6–13 K yielded the following result: $C_p/\mathrm{J\,K^{-1}\,mol^{-1}} = 3.4644 \times 10^{-3}(T/\mathrm{K})^3 + 5.5225 \times 10^{-5}(T/\mathrm{K})^5 - 5.0758 \times 10^{-7}(T/\mathrm{K})^7 + 1.2750 \times 10^{-9}(T/\mathrm{K})^9$. For the stable phases, standard thermodynamic functions are given in Table 2.

Table 2. Standard molar thermodynamic quantities of 3TCB.

T/K	$C^{\circ}_{p,m}$/J K^{-1} mol^{-1}	$[H^{\circ}_m(T)-H^{\circ}_m(0)]/T$/ J K^{-1} mol^{-1}	$S^{\circ}_m(T)-S^{\circ}_m(0)$/ J K^{-1} mol^{-1}	$-[G^{\circ}_m(T)-H^{\circ}_m(0)]/T$/ J K^{-1} mol^{-1}
10	5.19	1.28	1.68	0.40
20	22.88	7.39	10.32	2.94
30	42.50	15.85	23.34	7.49
40	60.69	24.81	38.09	13.28
50	76.28	33.59	53.35	19.76
60	89.78	41.88	68.51	26.63
70	101.03	49.54	83.21	33.67
80	112.56	56.69	97.44	40.75
90	124.47	63.56	111.38	47.83
		Phase transitions C5–C4–C3		
120	152.51	83.06	151.89	68.84
130	161.25	88.74	164.45	75.71
140	170.31	94.24	176.73	82.49
150	179.50	99.62	188.79	89.17
160	188.80	104.90	200.67	95.77
170	198.17	110.12	212.40	102.29
180	208.21	115.28	224.01	108.73
190	218.53	120.43	235.53	115.10
191.27	219.94	121.08	236.98	115.90
		Phase transition C3–C2		
191.27	228.73	127.89	243.79	115.90
200	235.99	132.45	254.16	121.71
210	243.96	137.58	265.87	128.30
220	252.26	142.60	277.41	134.81
230	260.77	147.55	288.81	141.26
240	269.76	152.46	300.10	147.64
250	279.13	157.34	311.30	153.96
259	288.33	161.71	321.32	159.61
		Phase transition C2–C1		
259	284.58	162.28	321.89	159.61
260	285.48	162.76	322.99	160.23
270	295.50	167.48	333.95	166.46
280	306.72	172.25	344.89	172.64
290	318.32	177.09	355.86	178.77
300	329.48	181.99	366.84	184.85
303.7	333.33	183.81	370.90	187.10
		Fusion C1–SmE		
303.7	349.04	206.93	394.03	187.10
310	354.28	209.88	401.26	191.38
320	362.32	214.52	412.63	198.11
330	370.27	219.12	423.90	204.78
340	378.59	223.69	435.08	211.39
350	387.82	228.24	446.18	217.94
360	397.31	232.80	457.24	224.43
362.92	400.20	234.13	460.45	226.32
		Phase transition SmE–I		
362.92	438.76	266.50	492.82	226.32
370	443.07	269.84	501.34	231.50

M=253.364 g mol^{-1}; p^o=101.325 kPa.

The rich polymorphism found for 3TCB is confirmed by IR spectroscopy (*20*). When compared to the simpler thermal behaviour of its homologous neighbour it indicates that the length of the alkyl chain affects considerably the cooperative dynamics of the intramolecular degrees of freedom in the SmE phase of *n*TCB series. The alkyl chain, as the most flexible part of the molecule in a well-packed arrangement, is supposed to play the role of a disordering (decorrelating) factor. In 3TCB it turns out to be insufficiently long for its conformational motions to disrupt the intermolecular correlations. These can trigger off a series of structural changes within the positionally-ordered crystalline phase, a feature absent for 4TCB and 5TCB.

Quenched phase

Deep supercooling of the SmE phase in 4TCB and 5TCB does not lead to vitrification (*13, 15*). The thermal behaviour of 3TCB obtained in the second measurement series, i.e. for the SmE phase quenched from above the melting temperature, points to the possibility that glass corresponding to the SmE phase is formed. The heat capacity values are observed to increase smoothly except for two areas around 222 K and 266 K where abrupt changes were detected. Interestingly, in both cases the heat capacity data display a sudden increase immediately above the transitions from phase C3 to C2 (191.27 K) and C2 to C1 (259 K), respectively. This close relation supports a hypothesis that at these points the same degrees of freedom which were "switched off" on cooling the stable crystalline phases at the transition points are activated on heating due to the increase of the amplitude of thermal fluctuations. IR spectroscopy yields additional evidence to corroborate that hypothesis (*20*). In the temperature range above a "softening" of the quenched phase of SmE and below the spontaneous transition towards the C2 phase, the heat capacity values exceed the values obtained by extrapolating the data for supercooling the SmE phase, cf. Figure 3. In this temperature range a substantial heat evolution (several $mK\,min^{-1}$ in terms of the temperature drift) was observed.

Usually around a glass transition, heat capacity shows a precipitous decrease on cooling and the characteristic enthalpy relaxation is observed in adiabatic conditions (*21, 22*). Although, in the case under study, the heat capacity jump was observed, the second feature was absent. The rate of spontaneous temperature change vs. temperature was

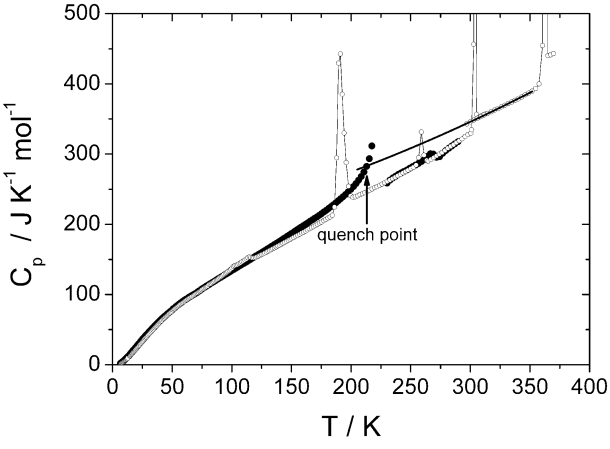

Figure 3. Linear extrapolation of the $C_p(T)$ data of the supercooled SmE (solid line) for the determination of the quench point. Open circles correspond to the crystal heat capacity data, whereas solid circles depict experimental heat capacity points obtained on heating the quenched phase.

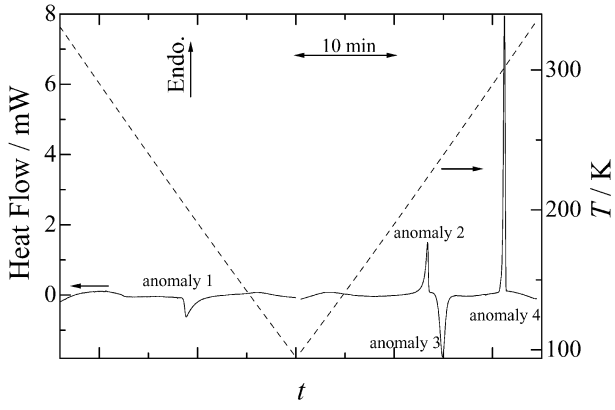

Figure 4. The DSC thermogram of 3TCB.

always positive. This may be due to the existence of some disorder not relaxed in glass transition and not removed in the spontaneous transformation at 222 K. The "softening" of the quenched phase of 3TCB seems to be a two-stage process with the intermediate phase observed prior to the complete relaxation to the stable crystal C1 phase. Non-monotonic behaviour of the heat capacity data during the next relaxation process around 270 K seems to support such interpretation. Let us also note that the observed relaxation process does not resemble a two-step relaxation observed for glass phases of SmG (*23, 24*). Thus the issue whether the quenched phase is glass or some metastable crystalline phase cannot be explained exclusively through the adiabatic calorimetry output.

To elucidate this point, a complementary DSC measurement was performed. The DSC thermogram is shown in Figure 4, and Table 3 provides the corresponding thermodynamic characteristics. There are four anomalies on the DSC curve. On cooling, one exothermic anomaly was observed at 205 K. This indicates that the anomaly is probably due to a phase transition from the supercooled SmE phase to a metastable crystalline phase as the presumed glass transition would be signalled by a step-like anomaly on the endothermic side. In the heating run three anomalies were detected. Anomaly 4 may be attributed to

Table 3. Anomalies revealed by the DSC measurement of 3TCB (cf. Figure 4).

Anomaly (i)	Onset temperature T_i/K	$\Delta_{trs}H_i$/ $kJ\,mol^{-1}$	$\Delta_{trs}S_i$/ $J\,K^{-1}\,mol^{-1}$
1	205	−2	−9.8
2	220	+1.9	+8.6
3	233	−4.8	−20.6
4	300	+7.0	+23.3

The minus (plus) sign corresponds to an exothermic (endothermic) anomaly.

C1–SmE phase transition, which is consistent with the adiabatic measurement. In addition, there are two other anomalies, the endothermic anomaly 2 at 220 K and exothermic anomaly 3 at 233 K.

The results obtained by adiabatic and differential calorimetry can be summarised by the *G–T* diagram shown in Figure 5. On cooling from 338 K, 3TCB undergoes a phase transition from SmE to a metastable unknown crystalline phase at 205 K (onset temperature) through the supercooled state of SmE. Heating this phase from 93 K triggers off a series of transitions: first to another metastable crystalline phase at 220 K, then, continuously, to another metastable crystalline phase at 233 K, next, to the stable crystalline phase C1 at 270 K and, finally, from the stable crystal to SmE at 303.7 K.

For the above reasons the transition temperature and other thermodynamic characteristics of the quenched phase cannot be determined in a straightforward way using the adiabatic calorimetry output. Yet the similarity of the heat capacity evolution on heating under adiabatic conditions (cf. Figure 3) to that of a glass transition suggests that the preliminary analysis of the data as if the quenched state were glassy should lead to approximate yet reasonable conclusions. As an approximation of the transition temperature to the quenched phase T_q we can use the counterpart of the so called "fictive" temperature, which will be defined by the intersection of the extrapolated $C_p(T)$ curves for the supercooled SmE and the quenched phase. By analogy to glass transitions, this corresponds to the temperature at which the quenched phase would be in metastable equilibrium if brought there instantaneously. The thermal evolution of the heat capacity of the supercooled SmE phase is extrapolated using a quadratic polynomial, as shown in Figure 3. The least squares fit to 20 data points of the corresponding cooling run, yields the following result change formula:

$$C_p/\mathrm{J\,K^{-1}\,mol^{-1}} = 179.614 + 317.182\times10^{-3}(T/\mathrm{K}) + 791.337\times10^{-6}(T/\mathrm{K})^2.$$

Using the above equation and the smoothed data of the quenched phase with the cubic spline procedure, the transition temperature was estimated to be $T_q \approx 213.2$K, which is in good agreement with the value estimated on the basis of the DSC measurement by the arithmetic mean $(T_1+T_2)/2 \approx 212.5$ K (cf. Table 3).

Figure 6 shows the heat capacity difference between the quenched SmE and stable crystalline states in 3TCB. Although the heat capacity of the quenched state becomes smaller than that of the stable crystalline state in the temperature range 80–120 K a broad maximum centred around 25 K is apparent. The least squares fit of the Schottky model (two-level system) to the data from the temperature range 6–80 K yielded the characteristic energy of 37 $\mathrm{cm^{-1}}$, which indicates that in the neutron inelastic scattering an excess phonon density may be expected around 4.6 meV, similar to that observed in some other materials (*25, 26*).

Standard thermodynamic functions

The standard thermodynamic functions obtained for the stable phases of 3TCB are given in Table 2. For the

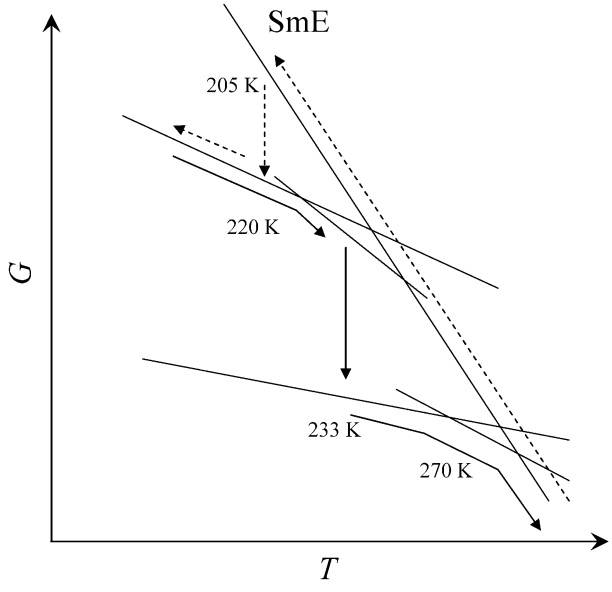

Figure 5. The *G–T* diagram indicated by calorimetric measurements for the quenched phase of 3TCB.

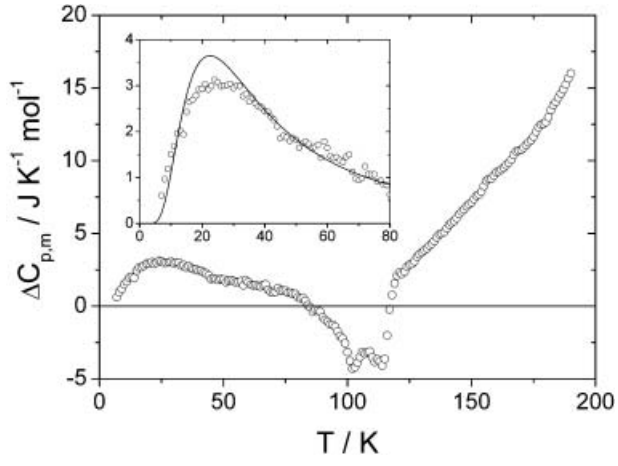

Figure 6. The heat capacity difference between the glassy and crystalline states plotted against temperature for 3TCB. The solid curve in the inset shows the calculated heat capacity for the two-level Schottky model with an energy gap of 37 $\mathrm{cm^{-1}}$.

quenched phase they were estimated on the basis of the four following assumptions. Most importantly, as implied by the DSC results, we assume that the quenched phase satisfies the third law of thermodynamics. Secondly, we approximate the phase transition point by the T_q estimated in the previous section. Next, we apply quadratic extrapolation of the supercooled SmE phase, as depicted in Figure 3. Finally, in order to estimate the values of C_p below 6 K we extrapolated the experimental values using a polynomial in temperature and matching it smoothly with the ensuing cubic spline fit. The least squares fitting to 13 first data points located in the temperature range 6–12 K yielded the following result: $C_p/\mathrm{J\,K^{-1}\,mol^{-1}} = 6.8024 \times 10^{-3}(T/\mathrm{K})^3 + 2.1179 \times 10^{-5}(T/\mathrm{K})^5 - 2.9500 \times 10^{-7}(T/\mathrm{K})^7 + 6.8111 \times 10^{-10}(T/\mathrm{K})^9$.

Figure 7 shows the entropy of the phases calculated for 3TCB. At the quench temperature, T_q, a drop of $10.2\,\mathrm{J\,K^{-1}\,mol^{-1}}$ is observed. This value agrees well with the entropy drop $\Delta_{trs}S_1 \approx -9.8\,\mathrm{J\,K^{-1}\,mol^{-1}}$ detected at the first DSC anomaly, which corroborates the presumption that as a result of the quench a metastable crystalline phase is formed. Next, knowing the entropy drop allows the corresponding enthalpy change to be estimated as equal to $2.18\,\mathrm{kJ\,mol^{-1}}$. Then, the difference in Gibbs energies of the stable crystalline and the quenched phase at $T = 0$ K, which is equal to the difference in enthalpies, is found to be equal to $2.71\,\mathrm{kJ\,mol^{-1}}$. In Figure 8, the enthalpy as function of temperature for the stable and metastable phases of 3TCB is depicted.

Whereas the value of the Gibbs energy difference is lower than its counterpart obtained for 4TCB, the residual entropy of the quenched phase of SmE of 3TCB turns out negligibly small. The latter fact indicates that the length of the alkyl chain represents a crucial factor serving as "entropy reservoir" and

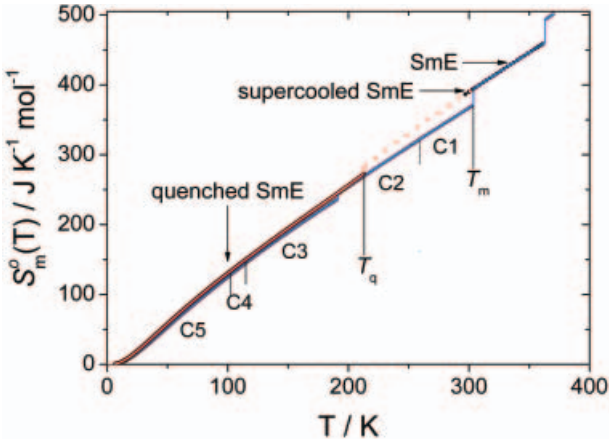

Figure 7. The entropy vs. temperature for the various phases of 3TCB.

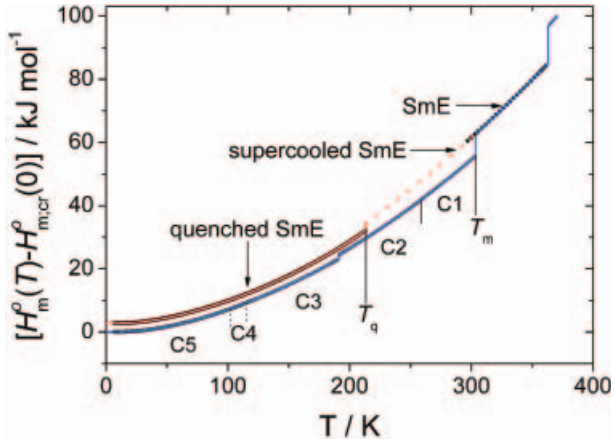

Figure 8. The enthalpy vs. temperature for the various phases of 3TCB.

shaping the phase patterns of 3TCB and its homologues. A similar phenomenon was observed for discotic mesogens BH(*n*) or thermotropic cubic mesogens, BABH(*n*) and ANBC(*n*) (*27*). However, elucidation of the exact nature of the order/disorder in the phases detected by calorimetry calls for further experimental evidence.

4. Conclusions

The results of the adiabatic calorimetry studies of the low member (propyl) of the *n*TCB homologous series have been reported. Rich solid-state polymorphism is revealed. Five crystalline phases and a transition to a metastable crystalline phase were detected. The phase transitions and the identification of the phases are corroborated by changes of IR spectra (*20*). In comparison to the phase pattern in 3TCB, the next higher member of the series (4TCB) exhibits a deeply supercooled disordered SmE phase and one stable crystalline phase (*13*), whereas in 5TCB two crystalline phases are found below the SmE phase (*15*). The large difference in thermal behaviour seems to indicate that the conformational motions of the alkyl chain play a critical role in the determination of a phase pattern. Further studies on other members of the *n*TCB homologous series could show the importance of the chain-length factor and how far conformational motions of odd alkyl chains are different from those of the even ones.

Acknowledgments

This work was supported by the JSPS Fellowship Program, ID No. P05736. Partial support was obtained from the grant of the Polish Ministry of Science and Higher Education No. 1P03B 60 28.

References

(1) Demus D.; Goodby J.; Gray W.; Spiess H.-W.; Vill V. *Handbook of Liquid Crystals*; Wiley-VCH: Weinheim, 1998; Vol. 1.
(2) Demus D. *Liquid Crystals*; Steinkopf Verlag: Darmstadt, 1994; p. 1.
(3) Diele S.; Tosch S.; Mahnke S.; Demus D. *Cryst. Res. Technol.* **1991**, *26*, 809–817.
(4) Dąbrowski R.; Przedmojski J.; Spadło A.; Dziaduszek J.; Tykarska M. *Phase Transitions* **2004**, *77*, 1103–1110.
(5) Urban S.; Przedmojski J.; Czub J. *Liq. Cryst.* **2005**, *32*, 619–624.
(6) Urban S.; Czupryński K.; Dąbrowski R.; Gestblom B.; Janik J.; Kresse H.; Schmalfuss H. *Liq. Cryst.* **2001**, *28*, 691–696.
(7) Drozd-Rzoska A.; Rzoska S.; Czuprynki K. *Phys. Rev. E* **2000**, *61*, 5355–5360.
(8) Massalska-Arodź M.; Schmalfuss H.; Witko W.; Kresse H.; Würflinger A. *Mol. Cryst. liq. Cryst.* **2001**, *366*, 221–227.
(9) Urban S.; Würflinger A. *Phys. Rev. E* **2005**, *72*, 021707.
(10) Vaz N.A.; Vaz M.J.; Doane J.W. *Phys. Rev. A* **1984**, *30*, 1008–1016.
(11) Richardson R.M.; Leadbetter A.J.; Carlile C.J.; Howells W.S. *Mol. Phys.* **1978**, *35*, 1697–1704.
(12) Richardson R.M.; Leadbetter A.J.; Frost J.C. *Mol. Phys.* **1982**, *45*, 1163–1191.
(13) Ishimaru S.; Saito K.; Ikeuchi S.; Massalska-Arodź M.; Witko W. *J. phys. Chem B* **2005**, *109*, 10020–10024.
(14) Jasiurkowska M.; Budziak A.; Czub J.; Urban S. *Acta phys. pol. A* **2006**, *110*, 795–805.
(15) Saito K., et al., in preparation.
(16) Czupryński K.; Dąbrowski R.; Przedmojski J. *Liq. Cryst.* **1989**, *4*, 429; Czupryński, K. *Mol. Cryst. liq. Cryst.* **1990,** *192,* 47–52.
(17) Yamamura Y.; Saito K.; Saitoh H.; Matsuyama H.; Kikuchi K.; Ikemoto I. *J. Phys. Chem. Solids* **1995**, *56*, 107–115.
(18) Saito K.; Amano M.; Yamamura Y.; Tojo T.; Atake T. *J. phys. Soc. Japan Lett.* **2006**, *75*, 033601.
(19) Nomoto K.; Atake T.; Chihara H. *J. phys. Soc. Japan* **1983**, *52*, 3475–3485.
(20) Jasiurkowska M., et al., in preparation.
(21) Sorai M. *Comprehensive Handbook of Calorimetry and Thermal Analysis*; John Wiley & Sons: Chichester, UK, 2004.
(22) Angell C.A. *Science* **1995**, *267*, 1924–1935.
(23) Yoshioka H.; Sorai M.; Suga H. *Mol. Cryst. liq. Cryst.* **1983**, *95*, 11–30.
(24) Sorai M.; Tani K.; Suga H. *Mol. Cryst. liq. Cryst.* **1983**, *97*, 365–386.
(25) Massalska-Arodź M.; Nakamoto T.; Wasiutyński T.; Mayer J.; Krawczyk J.; Sorai M. *J. chem. Thermodyn.* **2004**, *36*, 877–888.
(26) Mayer J.; Krawczyk J.; Massalska-Arodź M.; Natkaniec I.; Janik J.; Steinsvoll O. *Physica B* **2005**, *371*, 249–256.
(27) Sorai M.; Saito K. *Chem. Rec.* **2003**, *3*, 29–39.